





## Article

# A Novel, Quick, and Reliable Smartphone-Based Method for Serum PSA Quantification: Original Design of a Portable Microfluidic Immunosensor-Based System

Francisco Gabriel Ortega <sup>1,2</sup>, Germán E. Gómez <sup>3</sup>, Coral González-Martínez <sup>2</sup>, Teresa Valero <sup>1,4</sup>, José Expósito-Hernández <sup>1</sup>, Ignacio Puche <sup>1</sup>, Alba Rodríguez-Martínez <sup>2</sup>, María José Serrano <sup>1,2,5,6</sup>, José Antonio Lorente <sup>2,7</sup> and Martín A. Fernández-Baldo <sup>8,\*</sup>

- <sup>1</sup> IBS Granada, Instituto de Investigación Biosanitaria de Granada, 18012 Granada, Spain
  - <sup>2</sup> GENYO, Centre for Genomics and Oncological Research, Pfizer/University of Granada/Andalusian Regional Government, PTS Granada, Avenida de la Ilustración 114, 18016 Granada, Spain
  - <sup>3</sup> Instituto de Investigaciones en Tecnología Química (INTEQUI), Departamento de Química, Universidad Nacional de San Luis, CONICET, Chacabuco y Pedernera, San Luis D5700BWS, Argentina
  - <sup>4</sup> Department of Medicinal and Organic Chemistry, School of Pharmacy, University of Granada, Campus Cartuja s/n, 18071 Granada, Spain
  - <sup>5</sup> Integral Oncology Division, Virgen de las Nieves University Hospital, 18071 Granada, Spain
  - <sup>6</sup> Department of Pathological Anatomy, School of Medicine, University of Granada, 18071 Granada, Spain
  - <sup>7</sup> Lab. of Genetic Identification, Department of Legal Medicine & Toxicology and Physical Anthropology, School of Medicine, University of Granada, 18016 Granada, Spain
  - <sup>8</sup> INQUISAL, Departamento de Química, Universidad Nacional de San Luis, CONICET, Chacabuco 917, San Luis D5700BWS, Argentina
- \* Correspondence: mbaldo@unsl.edu.ar; Tel.: +54-266-443-0224



**Citation:** Ortega, F.G.; Gómez, G.E.; González-Martínez, C.; Valero, T.; Expósito-Hernández, J.; Puche, I.; Rodríguez-Martínez, A.; Serrano, M.J.; Lorente, J.A.; Fernández-Baldo, M.A. A Novel, Quick, and Reliable Smartphone-Based Method for Serum PSA Quantification: Original Design of a Portable Microfluidic Immunosensor-Based System. *Cancers* **2022**, *14*, 4483. <https://doi.org/10.3390/cancers14184483>

Academic Editors: Holger A. Siltmann and James Hicks

Received: 10 August 2022

Accepted: 6 September 2022

Published: 16 September 2022

**Publisher's Note:** MDPI stays neutral with regard to jurisdictional claims in published maps and institutional affiliations.



**Copyright:** © 2022 by the authors. Licensee MDPI, Basel, Switzerland. This article is an open access article distributed under the terms and conditions of the Creative Commons Attribution (CC BY) license (<https://creativecommons.org/licenses/by/4.0/>).

**Simple Summary:** Prostate cancer (PCa) is the most frequently diagnosed malignancy and second most common cause of cancer-related death in males. An early diagnosis is crucial to improve the prognosis. Prostate-Specific Antigen (PSA) is the most widely used biomarker for PCa, but this type of biomarker analysis is performed in centralized laboratories, delaying the diagnosis and initiation of treatment. Our team has developed a miniaturized platform for portable PSA quantification to overcome this shortcoming. It includes a microfluidic chip, immune capture of PSA by magnetic microbeads, and electrochemical quantification. The utilization of a micro-potentiostat allows PSA levels to be read on a smartphone in less than 30 min. This technique was found to offer a fast, easy, specific, sensitive, and reproducible method for PSA quantification. Further research is warranted to verify these findings and explore its potential application at all health care levels.

**Abstract:** We describe a versatile, portable, and simple platform that includes a microfluidic electrochemical immunosensor for prostate-specific antigen (PSA) detection. It is based on the covalent immobilization of the anti-PSA monoclonal antibody on magnetic microbeads retained in the central channel of a microfluidic device. Image flow cytometry and scanning electron microscopy were used to characterize the magnetic microbeads. A direct sandwich immunoassay (with horseradish peroxidase-conjugated PSA antibody) served to quantify the cancer biomarker in serum samples. The enzymatic product was detected at  $-100$  mV by amperometry on sputtered thin-film electrodes. Electrochemical reaction produced a current proportional to the PSA level, with a linear range from  $10$   $\text{pg mL}^{-1}$  to  $1500$   $\text{pg mL}^{-1}$ . The sensitivity was demonstrated by a detection limit of  $2$   $\text{pg mL}^{-1}$  and the reproducibility by a coefficient of variation of  $6.16\%$ . The clinical performance of this platform was tested in serum samples from patients with prostate cancer (PCa), observing high specificity and full correlation with gold standard determinations. In conclusion, this analytical platform is a promising tool for measuring PSA levels in patients with PCa, offering a high sensitivity and reduced variability. The small platform size and low cost of this quantitative methodology support its suitability for the fast and sensitive analysis of PSA and other circulating biomarkers in patients. Further research is warranted to verify these findings and explore its potential application at all healthcare levels.

**Keywords:** PSA; cancer biomarker; liquid biopsy; cancer diagnosis; magnetic microbeads; microfluidic immunosensor

## 1. Introduction

Liquid biopsies offer a noninvasive alternative to surgical biopsies [1] and are frequently used to study circulating tumor cells and cell-free DNA in blood samples [2]. They have long been employed to investigate protein biomarkers in venous blood [3], and more than 100 protein biomarkers have been developed over the past few decades for clinical diagnosis and evaluation of the therapeutic response or disease recurrence. The most widespread biomarkers approved by the USA Food and Drug Administration (FDA) and European Medicine Agency (EMA) [4] for urology and prostate cancer (PCa) disease include prostate-specific antigen (PSA) [5], carbohydrate antigen 125 (CA 125) [3], and carcinoembryonic antigen (CEA) [6], among others [7]. Despite the low sensitivity and specificity of these biomarkers, their increased levels in cancer provide clinicians with useful initial information about the disease status of patients [8]. However, the time taken by current techniques to analyze markers produces a delay in the delivery of results to clinicians [9,10]. This study proposes a portable and fast method for in situ biomarker analysis of PSA levels in patients with possible PCa. The protein PSA is specifically synthesized by the prostate, and its production is influenced not only by prostate size and androgen activity but also by prostate inflammation. PSA levels are generally very low in healthy males but elevated in the presence of prostatic disease, and they were found to be increased in 65% of patients with PCa [5]. The measurement of serum PSA levels is currently considered to be the most sensitive test to diagnose and stratify the severity of PCa.

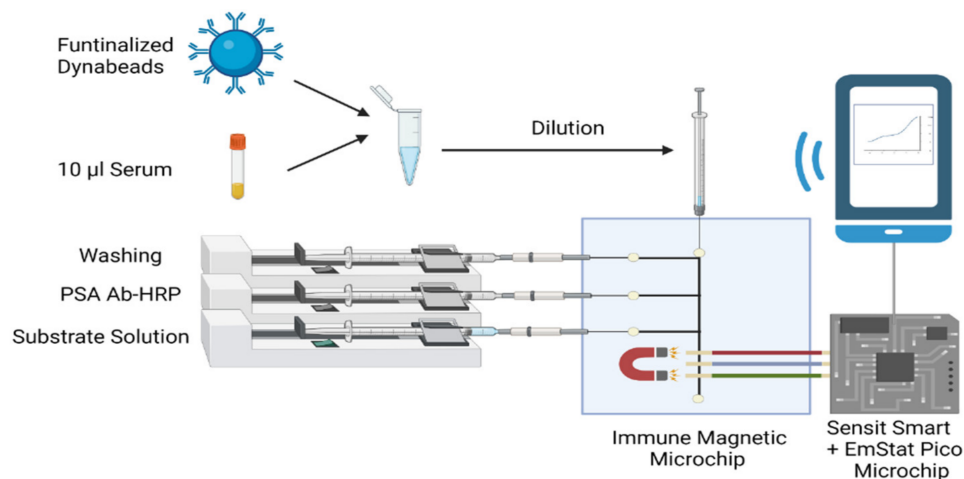
Radioimmuno assay (RIA) and enzyme-linked immunosorbent assay (ELISA) are currently used to determine PSA in the clinical setting, while fluorescent immunoassay, photoelectrochemical detection, and electrochemical immunosensors, among others, are used for research purposes [11–26]. In particular, electrochemical immunosensors have been proposed as a promising method for potential clinical application due to their high sensitivity and specificity [27–32]. They offer the possibility of performing simultaneous analyses and are easy to miniaturize, providing a simple analysis technique at a lower cost [33–37]. Immune-electrochemical sensors are highly specific due to the affinity between antibody and antigen, while the electrochemical signal induced by the hybridization of antigen–antibody is the measurable signal that correlates with the protein concentration [33,35]. The coupling of immunosensors with microfluidic systems provides additional advantages, including smaller sample volumes, faster turnaround times, and lower costs [38–43]. These systems contain microchannels for transporting fluids and some or all of the components required for an immunoassay [38–43]. It has been demonstrated that the combination of microfluidic technology with electrochemical sensing improves the overall detection capability [39,40,43].

Microfluidic immunosensors have shown promise for the analysis of tumoral biomarkers. Various types of particles, such as magnetic microbeads, have recently been incorporated to amplify the reaction surface and sensor response, enhancing the sensitivity of biomarker detection [39,44,45]. The utilization of these nanoparticles as solid support for electrochemical reaction has been proposed for the development of PSA sensors [46–48]. Further research is required to design and manufacture this type of biosensor, and there is a need to develop a portable platform that allows in situ analysis in real conditions and not only in the laboratory setting. Further steps to be taken include benchmarking the biosensor against established methodologies, creating a user-friendly interface for utilization by non-specialists, and testing the device in the field to obtain feedback from users.

The present study describes a microfluidic chip for the immune-magnetic capture and immuno-electrochemical quantification of PSA [11,12]. This microfluidic immunosensor

is coupled to a platform designed for smartphones and the inexperienced user, called the *Smartphone FAST-PSA tool*. Interestingly, this system can be readily adapted for the determination of other biomarkers by changing the working solutions (Figure 1A). In this study, the analytical parameters of this device were tested in reference samples, and it was used to measure PSA levels in 96 blood samples obtained at different time points from 50 donors with PCa, comparing findings with the results of gold standard methodologies.

**A.**



**B.**

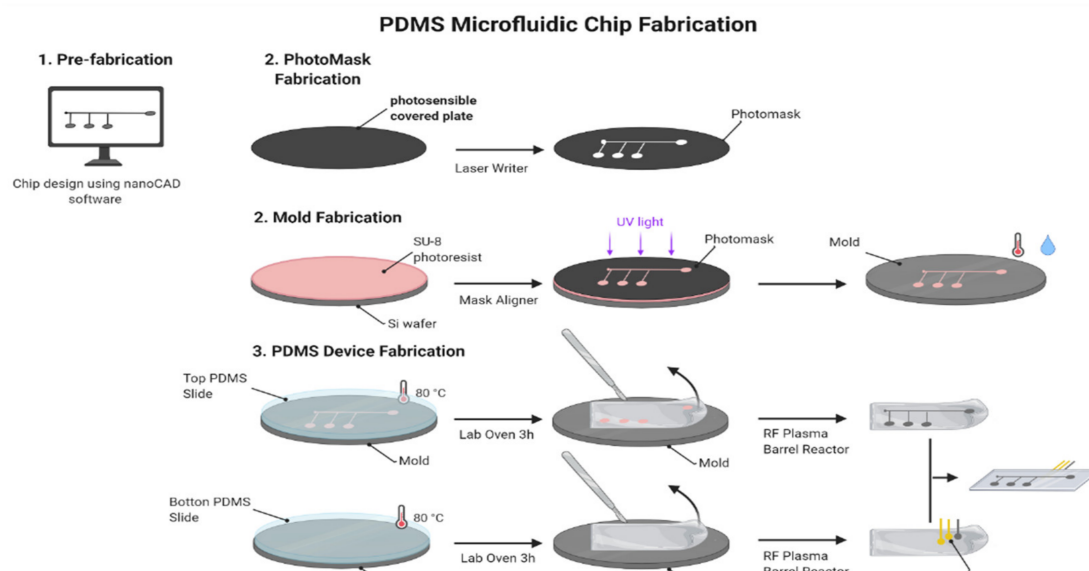


**Figure 1.** (A) Schematic representation of the *Smartphone FAST-PSA tool*. (B) Schematic representation of the microfluidic chip fabrication.

## 2. Materials and Methods

### 2.1. Apparatus

Fabrication of the microfluidic chip and electrodes utilized a  $\mu$ PG 101 desk-top laser writer (Heidelberg Instruments, Heidelberg, Germany), Karl Suss MA6 Mask Aligner (Suss Microtec, Garching, Germany), Diener Asher RF plasma barrel reactor (Diener electronic,

Ebhausen, Germany) and AJA ATC-1800 sputtering system (AJA International Inc., MA, USA). The Amnis ImageStream X Mk II imaging cytometer (Luminex, Austin, TX, USA) and Zeiss GEMINI high-resolution Scanning Electron Microscope (SEM) were employed to characterize the microbeads. A Sensit Smart Potentiostat (Palm Sens, Houten, The Netherlands) was used for amperometric detection.

### 2.2. Electrode Fabrication

The structured electrodes were fabricated as previously described [49]. Briefly, pre-stressed polystyrene sheets (PS) were washed with isopropanol, ethanol, and water, dried under nitrogen flow, and coated with a SU-8 photoresist (MicroChem, Newton, MA, USA) layer of 2  $\mu\text{m}$  thickness. Then, self-adhesive vinyl was cut with the specific patterns and dimensions of the working (WE), auxiliary (AE), and reference (RE) electrodes and placed onto the PS-coated slide. Gold and platinum were deposited using the sputtering system at a deposition rate of  $\sim 1 \text{ \AA/s}$  (100 nm) for gold and  $\sim 0.1 \text{ \AA/s}$  (150 nm) for platinum. Next, the vinyl was removed, and the PS slides were placed in an oven at 160  $^{\circ}\text{C}$  to shrink the PS. Finally, the electrodes were lifted by dissolving the PS in an acetone bath and were conserved in acetone until further use.

### 2.3. PDMS Microfluidic Device Fabrication

The fabrication of this device was performed according to the protocol described by Saem et al. [50]. Briefly, The microfluidic pattern was designed with nanoCad (Nanosoft, London, UK) and drawn on glass coated with a photo-sensitive material to create the mask by soft lithography as described by Saem et al. [50]. The mask was then aligned over the SU-8 (photoresist)-coated silicon wafer and exposed to UV light in a  $\mu\text{PG}$  101 desk-top laser writer to create the mold. Next, after washing the non-polymerized photoresist, the mold was placed on a petri dish and coated with PDMS prepolymer previously mixed with the curing agent (Down, Midland, TX, USA). Air bubbles were removed by exposing the molds to multiple vacuum cycles. The PDMS was cured at 80  $^{\circ}\text{C}$  for 3 h and then cut and peeled from the mold for cleaning and activation with  $\text{O}_2$  plasma. Finally, the upper slide with the microfluidic channel was pressed against the lower slide with the electrodes (Figure 1B).

### 2.4. Characterization of the Solid Support

Commercial Dynabeads-COOH (Invitrogen<sup>TM</sup>, Waltham, MA, USA) were purchased from ThermoFisher Scientific. For characterization of their size, morphology, and concentration by imaging flow cytometry, the microbeads were diluted 1/100 in 10 mM phosphate-buffered saline (PBS) with pH of 7.20 at 40 mm/s, and each event was photographed at 60 $\times$  magnification using ImageStream equipment. The IDEAS software was used for the data analysis. For characterization by SEM, the microbeads were fixed in a solution of PBS with 4% paraformaldehyde and 1% glutaraldehyde for 24 h and were then washed in PBS followed by incubation in 2% osmium tetroxide for 1 h. Microbeads were then fully dehydrated in serial ethanol solutions. Finally, the dry sample was sprinkled onto slide glass and metalized for photography with the Zeiss Gemini scanning electron microscope.

### 2.5. Immobilization of the Anti-PSA in Magnetic Microbeads

A suspension of homogenized commercial COOH microbeads (Thermo Scientific, Waltham, MA, USA) was washed twice with 0.1 M NaOH solution for 10 min and twice with  $\text{H}_2\text{O}$  for 10 min. The beads were then magnetically separated to remove the supernatant, followed by activation of the surface carboxylic groups of the microbeads in a freshly prepared 1-Ethyl-3-(3-dimethylaminopropyl) carbodiimide (EDC) solution for 30 min. The microbeads were then washed twice with 2-(N-morpholino) ethanesulfonic acid (MES) buffer before incubation in a solution with excess PSA antibody (PSA-Ab) in MES buffer. Next, the microbeads were incubated in a 1 M ethanolamine solution to block residual activated groups. Finally, they were washed once with 0.1 M Tris-HCl buffer (pH 7.2)



and twice with PBS. The functionalized microbeads were stored at 4 °C in PBS until their utilization.

### 2.6. Analytical Procedure for PSA Determination

All solutions were injected at a flow rate of  $2 \mu\text{L min}^{-1}$ . A schematic representation of this procedure is depicted in Figure 1A. Briefly,  $1 \times 10^6$  of PSA-Ab-MBs were dissolved in 50  $\mu\text{L}$  of 1% BSA, 0.1% Tween, and 2% goat serum in PBS and incubated for 10 min. Next, 10  $\mu\text{L}$  of circulating plasma samples were added and incubated in a shaker for 15 min at room temperature. The sample was then collected into a 0.1 mL syringe and manually injected into the central channel of the microfluidic system. Next, the beads were washed with 10 mM PBS pH 7.20 for 4 min, and HRP-conjugated anti-PSA (diluted 1000-fold with 10 mM PBS pH 7.20) was then added for a further 5 min, followed by another wash for 4 min. Finally, the enzyme substrate (1 mM  $\text{H}_2\text{O}_2$  + 1 mM 4-TBC in 10 mM phosphate-citrate buffer pH 5.00) was injected, and the electrochemical reaction was detected at  $-100$  mV by amperometry using the PStouch app for Android and PStace for Windows (Palm Sens, Houten, The Netherlands).

### 2.7. Blood Sample Collection

The study was approved by the Ethical Committee of Virgen de las Nieves University Hospital and complied with the principles of the Declaration of Helsinki. Written informed consent was obtained for all of the samples. The patients were enrolled and followed at the Urology and Oncology Departments of the hospital. Table S1 (Supplementary Materials) exhibits the clinical data of the study participants.

## 3. Results

### 3.1. Characterization and Functionalization of the Solid Support

Commercial Magnetic MBs Dynabeads<sup>TM</sup> were characterized by image cytometry and SEM. A total of  $1 \times 10^4$  particles were photographed and analyzed by Image Cytometer ImageStream<sup>TM</sup>, revealing the circular and homogeneous beads depicted in Figure 2A,B. Image analysis using IDEAS software showed a mean circularity of  $0.9898 \pm 0.00549$  (range 0.03502), a mean diameter of  $2.787 \pm 0.06618 \mu\text{m}$  (range 0.408  $\mu\text{m}$ ) and a mean area of  $6.1 \pm 0.2913 \mu\text{m}^2$  (range, 1.778  $\mu\text{m}^2$ ). SEM images also depicted highly homogenous spherical particles with a diameter of around 2.7  $\mu\text{m}$  and marked surface rugosity (Figure 2C).

The microbeads were functionalized with antibodies against human PSA, as described in the Methods section. The amount of bound microbead antibody was calculated by determining the initial and final anti-PSA antibody concentrations before and after the coupling reaction (Figure S1A). An excess of antibody was observed in the initial solution and a reduction of  $41.22 \pm 0.13\%$  after the coupling reaction (Figure S1B).

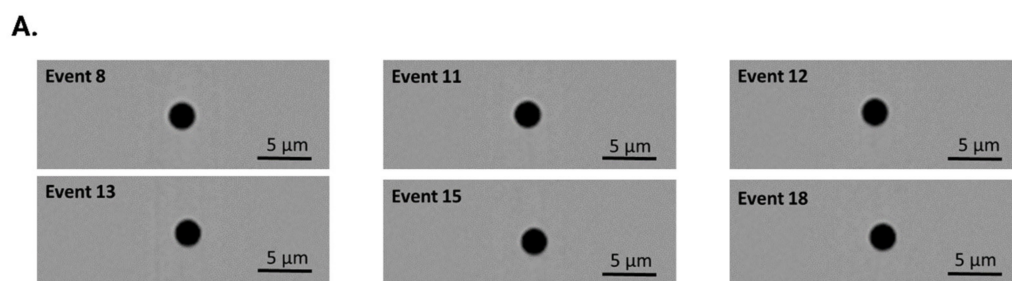
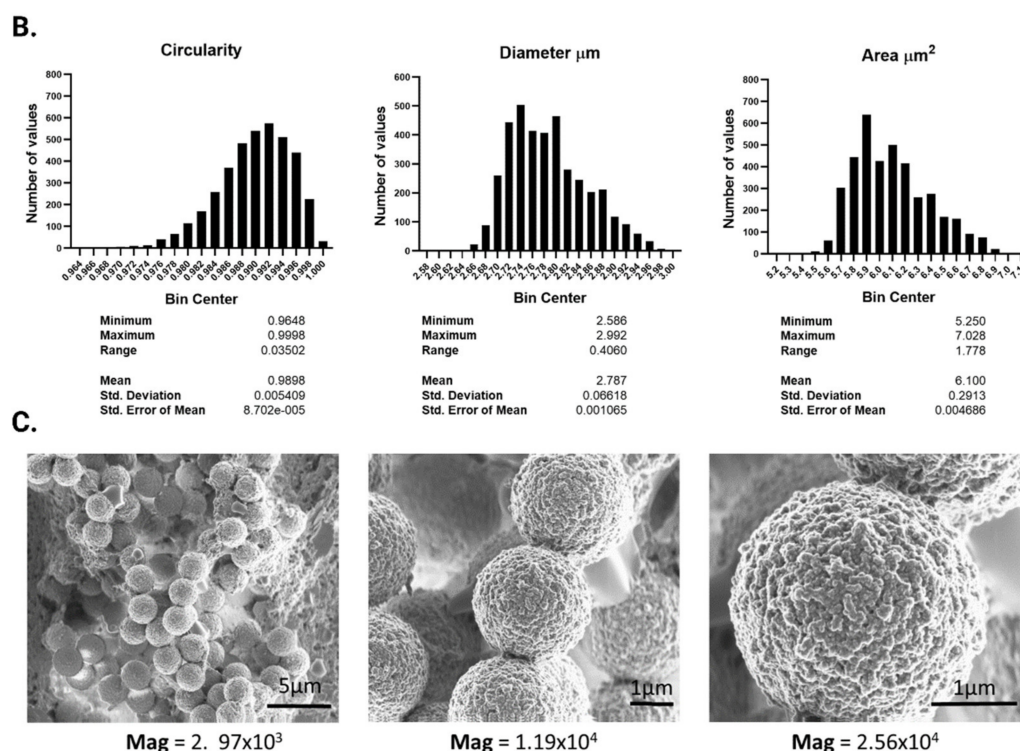


Figure 2. Cont.



**Figure 2.** (A) Representative images obtained by image cytometry. (B) Histograms showing the frequency distribution of circularity, with perfect circularity = 1, diameter expressed in  $\mu\text{m}$ , and area expressed in  $\mu\text{m}^2$ . (C) Representative SEM micrographs of the Dynabeads<sup>TM</sup>, obtained at several magnifications (Mag).

### 3.2. Optimization of Experimental Variables

A control dilution of 800 pg mL was used for the optimization of experimental variables<sup>-1</sup>. The optimal flow rate was determined by evaluating the current intensity at different flow rates. As shown in Figure 3A, the flow rates from 1 to 2.5  $\mu\text{L min}^{-1}$  had little effect on the signal obtained, which was markedly reduced at flow rates > 3  $\mu\text{L min}^{-1}$ . The optimal pH was then determined by testing solutions in a pH range of 4–7, observing the maximum current intensity at pH 5 (Figure 3B).

### 3.3. Quantitative Determination of PSA Biomarker in the Microfluidic Immunosensor

The *Smartphone FAST-PSA tool* platform was used to determine the current of serial PSA dilutions under the optimized conditions. The linear regression equation was  $i \text{ (nA)} = 9.534 + 0.230 \times \text{CPSA}$ , with linear regression coefficient of 0.997. The methodology shows a linear correlation of 10–1500  $\text{pg mL}^{-1}$  (Figure 4A).

Intra-assay and inter-assay coefficients of variation (CVs) were then determined in solutions of 10, 800, and 1600  $\text{pg mL}^{-1}$  of PSA (five determinations in each), finding an intra-assay CV of 3.82% at 800  $\text{pg mL}^{-1}$  and an inter-assay CV of 5.24% at 800  $\text{pg mL}^{-1}$  (Table 1).

Next, a commercial ELISA test was used to plot the absorbance changes against the corresponding PSA concentration of serially diluted samples. The linear regression equation was  $A = 0.033 + 0.001 \times \text{CPSA}$ , with a regression coefficient of 0.947 and CV of 6.47% for the determination of 800  $\text{pg mL}^{-1}$  PSA (five replicates), a lower precision than obtained with the present platform.

The limit of detection (LOD) was defined as the lowest concentration yielding a signal three times the standard deviation of the blank. The LOD was 8  $\text{pg mL}^{-1}$  for the ELISA test, higher (less sensitive) than the LOD of 2  $\text{pg mL}^{-1}$  for the present platform.

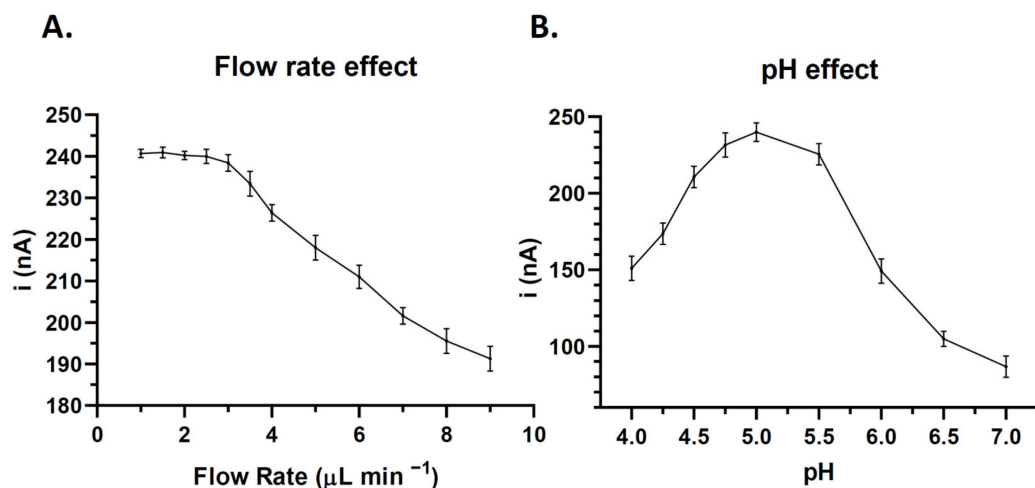


**Figure 3.** (A) Correlation between flow rates of electrochemical substrate dilution and the current generated on the electrode surface at  $-100$  mV. Each dot represents the mean of 5 determinations and the error bar corresponds to the standard deviation. (B) Correlation between the pH of electrochemical substrate dilution and the current generated on the electrode surface at  $-100$  mV. Each dot represents the mean of 5 determinations and the error bar corresponds to the standard deviation.

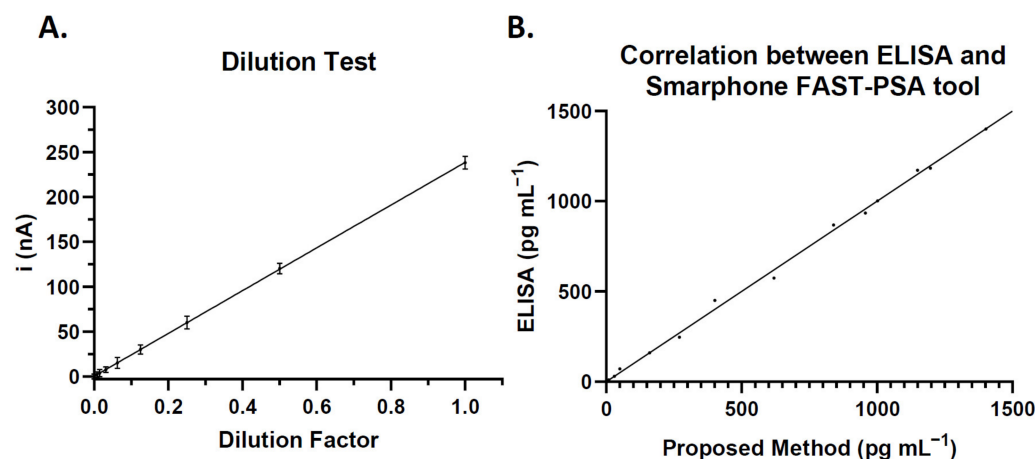


**Figure 4.** (A) Correlation between serial dilution of PSA in 10 mM PBS (pH 7.20) and the current level determined by the method. Each value is the mean of five determinations, and error bars represent standard deviations. (B) Correlation between *Smartphone FAST-PSA tool* platform and commercial ELISA.

**Table 1.** Intra-assay precision (five measurements in the same run for each control sample) and inter-assay precision (five measurements for each control sample, repeated for three consecutive days).

<sup>a</sup> Control Sample	Intra-Assay		Inter-Assay	
	Mean	CV%	Mean	CV%
10	9.98	2.71	10.04	4.46
800	799.95	3.82	800.02	5.42
1200	1199.98	3.50	1200.03	6.16

<sup>a</sup> pg/mL PSA.

The proposed analytical methodology was compared with a commercial ELISA, using both to analyze 15 samples with different PSA levels. The slopes obtained were close to 1 ( $r = 0.997$ ), indicating a good correlation of the two methods (Figure 4B).

### 3.4. Clinical Performance of the Smartphone FAST-PSA Tool Platform for PSA Analysis

The specificity and selectivity of the platform to determine PSA in serum were tested by spiking a pool of serum from healthy donors with PSA at different dilutions. As shown in Figure 5A, the added PSA was fully correlated with the concentration measured by the sensor in the platform. Linear regression analysis showed a slope of  $1.002 \pm 0.0024$  with 95% confidence interval (CI) of 0.9972 to 1.007 and slope intercept at  $1.695 \pm 0.0982$  (95% CI, 1.492 to 1.899), the baseline concentration in the serum pool from the donors. Next, 96 liquid biopsy samples from 50 patients underwent different treatments at baseline (before treatment) and at 6 and 12 weeks. The results were also validated against the two gold standard methods routinely used in the hospital laboratory, RIA and ELISA, finding an excellent correlation (Figure 5B), with a linear regression slope of  $1.050 \pm 0.0108$  (95% CI, 1.030 to 1.071).

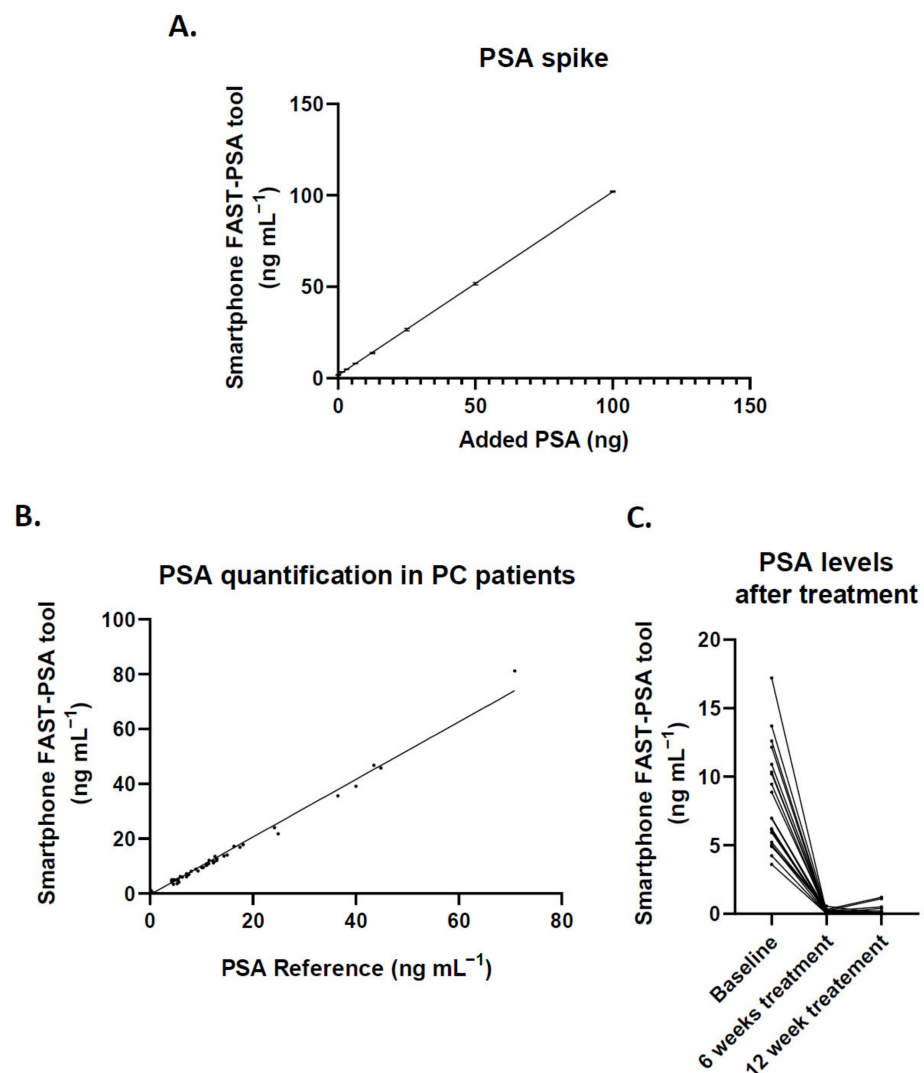


**Figure 5.** (A) The specificity and accuracy of the methodology were determined by spiking serum from healthy donors with known amounts of PSA; this graph depicts the mean of three independent experiments, with an error bar representing the standard deviation (SD). (B) Comparison of PSA data between the *Smartphone FAST-PSA tool* and laboratory testing (RIA or ELISA). Each dot represents the same sample analyzed by both methods. (C) Determination of the usefulness of the tool for the follow-up of patients with PCa; the graph depicts PSA levels at baseline (before treatment) and at 6 and 12 weeks of chemical castration treatment.

A test was also conducted of the platform's capacity to monitor the effects of therapy on PSA levels, which were determined in 22 patients with PCa at baseline and after 6 and 12 weeks of chemical castration treatment (Figure 5C). The PSA levels were markedly reduced by the treatment and were slightly lower after 6 versus 12 weeks of treatment.

#### 4. Discussion

This study presents a novel microfluidic portable immunosensor-based method for the fast and reliable in situ quantification of PSA by clinicians using a smartphone.

The need to avoid any delay in the diagnosis of PCa has led to the development of rapid portable platforms that allow PSA levels to be determined in the clinical setting. Barbosa et al. [51] tested a fluoropolymer microfluidic device to quantify PSA using a smartphone and reported promising results, although the influence of ambient light on measurements limits its usefulness as a standardized methodology for application across centers with different lighting. This possibility of inter-assay error is markedly reduced by combining electrochemistry on a microfluidic chip. Mavrikou et al. [52] developed a biosensor whose membrane potential is modified by engineered cells in the presence of PSA, indicating a high ( $>4 \text{ ng mL}^{-1}$ ) or low ( $<4 \text{ ng mL}^{-1}$ ) PSA level. However, the use of cells as the sensing element limits the ease of use and the storage and portability of the device. For their part, Srinivasan et al. [53] coupled a gold nanoshell with anti-PSA antibody to obtain a colorimetric reaction on strip paper read in a custom cube but achieved only a semi-quantitative analysis. Numerous proposals for electrochemical PSA detection are described in a recent review [54]; however, the present device is the first PSA biosensor integrated within a fully portable platform that can be connected to a smartphone through the incorporation of a miniaturized potentiostat. The software for operating this device is highly intuitive and can be downloaded free from <https://www.palmsens.com/software/pstouch/> (accessed on 11 June 2020), allowing measurements to be run, standard curves to be loaded and saved, and peaks to be analyzed and manipulated. It also permits the sharing of results via email or any other platform and supports other types of accessories (e.g., syringe pumps). Finally, the supplier allows for the modification and personalization of the interface using open code format.

There are certain limitations in the utilization of PSA as a biomarker of PCa, with reports of false positives and a resulting overdiagnosis and overtreatment of patients. However, the present platform can be simply adapted to detect other biomarkers by replacing the syringe content with different reaction components (Figure 1A). The system can even be modified on demand to include new biomarkers or other proteins found to be relevant for cancer diagnosis and treatment. Furthermore, the incorporation of functionalized magnetic microbeads offers high versatility, reduces incubation and washing times, and increases the reaction surface of the sputtered electrodes, thereby enhancing the sensitivity of the biosensor [39,44]. In summary, the device provides a reliable quantification of PSA that would be easy to implement at all health-care levels.

#### 5. Conclusions

The *Smartphone FAST-PSA tool* is a novel portable platform for smartphones based on the immunomagnetic immobilization of PSA and its immuno-electrochemical quantification. Its performance was tested in serial dilutions of PSA and in human samples, yielding the same values as those obtained by the gold standard methods. Advantages of this microfluidic immunosensor include its stability and its high selectivity and sensitivity, attributable to the immobilization of monoclonal antibodies by the magnetic microbeads. It provides the clinician with a rapid and reliable measurement of PSA levels and its fabrication is not costly, further supporting its potential for clinical implementation at all healthcare levels.



**Supplementary Materials:** The following supporting information can be downloaded at: <https://www.mdpi.com/article/10.3390/cancers14184483/s1>, Figure S1. Schematic representation of the chemical reaction for coupling of the anti-PSA antibody to the magnetic microbeads and assessment of coupling efficiency; Table S1. Data of recruited patients; Table S2. PSA levels obtained by the proposed platform.

**Author Contributions:** Conceptualization, F.G.O. and M.A.F.-B.; methodology, F.G.O., G.E.G., C.G.-M. and A.R.-M.; software, F.G.O.; validation, J.E.-H. and I.P.; formal analysis, M.J.S., J.A.L. and T.V.; resources, M.J.S., J.A.L. and M.A.F.-B.; writing—original draft preparation, F.G.O. and M.A.F.-B.; writing—review and editing, T.V., M.J.S. and J.A.L.; supervision, J.E.-H.; project administration, I.P. and A.R.-M.; funding acquisition, M.J.S. and M.A.F.-B. All authors have read and agreed to the published version of the manuscript.

**Funding:** Funding is acknowledged from the Universidad Nacional de San Luis (PROICO 22/Q241), from the Agencia Nacional de Promoción Científica y Tecnológica (PICT 2018-04443, PICT-2015-2246, PICT-2015-1575, PICT-2014-1184, PICT-2014-0375 and PICT-2018-04443), from Consejo Nacional de Investigaciones Científicas y Técnicas (CONICET) (Argentina) (PIP 11220150100004CO), from GENYO, Centre for Genomics and Oncological Research: Pfizer-University of Granada, Andalusian Regional Government (Granada, Spain), from ISCIII Health Research Institute (P17/00989), ‘La Caixa’ Foundation. F.G.O. is funded by the Health and Family Secretariat of the Andalusian Regional Government. T.V. is funded by H2020-MSCA-IF-2019-895664. C.G. and A.R. are supported by PhD program from the Spanish Ministry of Education. G.E.G. and M.F.B. are members of the Carrera del Investigador Científico-Consejo Nacional de Investigaciones Científicas y Técnicas (CIC-CONICET).

**Institutional Review Board Statement:** The study was conducted according to the guidelines of the Declaration of Helsinki, and approved by the Research Ethical Committee of Granada, CEI-GRANADA (protocol code CYTOF-PROSTATA CE) on 28 March 2017.

**Informed Consent Statement:** Yes, all protocols were performed according to the Helsinki declaration, and all enrolled volunteers signed their informed consent.

**Data Availability Statement:** The data presented in this study are available in the Supplementary Materials and on request from the corresponding author.

**Conflicts of Interest:** The authors declare no conflict of interest.

## References

1. Lianidou, E.; Pantel, K. Liquid biopsies. *Genes Chromosom. Cancer* **2019**, *58*, 219–232. [[CrossRef](#)] [[PubMed](#)]
2. Ignatiadis, M.; Sledge, G.W.; Jeffrey, S.S. Liquid biopsy enters the clinic—Implementation issues and future challenges. *Nat. Rev. Clin. Oncol.* **2021**, *185*, 297–312. [[CrossRef](#)]
3. Jacobs, E.L.; Haskell, C.M. Clinical use of tumor markers in oncology. *Curr. Probl. Cancer* **1991**, *15*, 301–350. [[CrossRef](#)]
4. Chatterjee, S.K.; Zetter, B.R. Cancer biomarkers: Knowing the present and predicting the future. *Futur. Oncol.* **2005**, *1*, 37–50. [[CrossRef](#)]
5. Harris, R.; Lohr, K.N. Screening for prostate cancer: An update of the evidence for the U.S. Preventive Services Task Force. *Ann. Intern. Med.* **2002**, *137*, 917–929. [[CrossRef](#)] [[PubMed](#)]
6. Hall, C.; Clarke, L.; Pal, A.; Buchwald, P.; Eglinton, T.; Wakeman, C.; Frizelle, F. A Review of the Role of Carcinoembryonic Antigen in Clinical Practice. *Ann. Coloproctol.* **2019**, *35*, 294. [[CrossRef](#)] [[PubMed](#)]
7. Mancini, M.; Zazzara, M.; Zattoni, F. Stem cells, Biomarkers and Genetic Profiling: Approaching future challenges in Urology. *Urologia J.* **2016**, *83*, 4–13. [[CrossRef](#)]
8. Diamandis, E.P.; Bast, R.C.; Gold, P.; Chu, T.M.; Magnani, J.L. Reflection on the discovery of carcinoembryonic antigen, prostate-specific antigen and carbohydrate antigens ca125 and ca19.9. *Clin. Chem.* **2013**, *59*, 22. [[CrossRef](#)]
9. Skrzypczyk, H.J.; Verdier, P. Bioanalytical Assays: RIA/EIA. In *Drug Discovery and Evaluation: Safety and Pharmacokinetic Assays*, 2nd ed.; Springer: Berlin/Heidelberg, Germany, 2013; pp. 869–886. [[CrossRef](#)]
10. Li, W.; Shao, B.; Liu, C.; Wang, H.; Zheng, W.; Kong, W.; Liu, X.; Xu, G.; Wang, C.; Li, H.; et al. Noninvasive Diagnosis and Molecular Phenotyping of Breast Cancer through Microbead-Assisted Flow Cytometry Detection of Tumor-Derived Extracellular Vesicles. *Small Methods* **2018**, *2*, 1800122. [[CrossRef](#)]
11. Zhu, Q.; Li, C.; Chang, H.; Jiang, M.; Sun, X.; Jing, W.; Huang, H.; Huang, D.; Kong, L.; Chen, Z.; et al. A Label-Free Photoelectrochemical Immunosensor for Prostate Specific Antigen Detection Based on Ag<sub>2</sub>S Sensitized Ag/AgBr/BiOBr Heterojunction by in-Situ Growth Method. *Bioelectrochemistry* **2021**, *142*, 107928. [[CrossRef](#)]

12. Darvishi, E.; Ehzari, H.; Shahlaei, M.; Behbood, L.; Arkan, E. The Electrochemical Immunosensor for Detection of Prostatic Specific Antigen Using Quince Seed Mucilage-GNPs-SNPs as a Green Composite. *Bioelectrochemistry* **2021**, *139*, 107744. [[CrossRef](#)] [[PubMed](#)]
13. Assari, P.; Rafati, A.A.; Feizollahi, A.; Joghani, R.A. Fabrication of a Sensitive Label Free Electrochemical Immunosensor for Detection of Prostate Specific Antigen Using Functionalized Multi-Walled Carbon Nanotubes/Polyaniline/AuNPs. *Mater. Sci. Eng. C* **2020**, *115*, 111066. [[CrossRef](#)] [[PubMed](#)]
14. Shamsazar, A.; Asadi, A.; Seifzadeh, D.; Mahdavi, M. A Novel and Highly Sensitive Sandwich-Type Immunosensor for Prostate-Specific Antigen Detection Based on MWCNTs-Fe<sub>3</sub>O<sub>4</sub> Nanocomposite. *Sens. Actuators B Chem.* **2021**, *346*, 130459. [[CrossRef](#)]
15. Chen, S.; Xu, L.; Sheng, K.; Zhou, Q.; Dong, B.; Bai, X.; Lu, G.; Song, H. A Label-Free Electrochemical Immunosensor Based on Facet-Controlled Au Nanorods/Reduced Graphene Oxide Composites for Prostate Specific Antigen Detection. *Sens. Actuators B Chem.* **2021**, *336*, 129748. [[CrossRef](#)]
16. Yang, C.; Guo, Q.; Lu, Y.; Zhang, B.; Nie, G. Ultrasensitive “Signal-on” Electrochemiluminescence Immunosensor for Prostate-Specific Antigen Detection Based on Novel Nanoprobe and Poly(Indole-6-Carboxylic Acid)/Flower-like Au Nanocomposite. *Sens. Actuators B Chem.* **2020**, *303*, 127246. [[CrossRef](#)]
17. Han, L.; Wang, D.; Yan, L.; Petrenko, V.A.; Liu, A. Specific Phages-Based Electrochemical Impedimetric Immunosensors for Label-Free and Ultrasensitive Detection of Dual Prostate-Specific Antigens. *Sens. Actuators B Chem.* **2019**, *297*, 126727. [[CrossRef](#)]
18. Zhao, L.Z.; Fu, Y.Z.; Ren, S.W.; Cao, J.T.; Liu, Y.M. A Novel Chemiluminescence Imaging Immunosensor for Prostate Specific Antigen Detection Based on a Multiple Signal Amplification Strategy. *Biosens. Bioelectron.* **2021**, *171*, 112729. [[CrossRef](#)]
19. Medetalibeyoglu, H.; Kotan, G.; Atar, N.; Yola, M.L. A Novel and Ultrasensitive Sandwich-Type Electrochemical Immunosensor Based on Delaminated MXene@AuNPs as Signal Amplification for Prostate Specific Antigen (PSA) Detection and Immunosensor Validation. *Talanta* **2020**, *220*, 121403. [[CrossRef](#)]
20. Ehzari, H.; Amiri, M.; Safari, M. Enzyme-Free Sandwich-Type Electrochemical Immunosensor for Highly Sensitive Prostate Specific Antigen Based on Conjugation of Quantum Dots and Antibody on Surface of Modified Glassy Carbon Electrode with Core-Shell Magnetic Metal-Organic Frameworks. *Talanta* **2020**, *210*, 120641. [[CrossRef](#)]
21. Thunkhamrak, C.; Chuntib, P.; Ounnunkad, K.; Banet, P.; Aubert, P.H.; Saianand, G.; Gopalan, A.I.; Jakmune, J. Highly Sensitive Voltammetric Immunosensor for the Detection of Prostate Specific Antigen Based on Silver Nanoprobe Assisted Graphene Oxide Modified Screen Printed Carbon Electrode. *Talanta* **2020**, *208*, 120389. [[CrossRef](#)]
22. Choosang, J.; Khumngern, S.; Thavarungkul, P.; Kanatharana, P.; Numnuam, A. An Ultrasensitive Label-Free Electrochemical Immunosensor Based on 3D Porous Chitosan-Graphene-Ionic Liquid-Ferrocene Nanocomposite Cryogel Decorated with Gold Nanoparticles for Prostate-Specific Antigen. *Talanta* **2021**, *224*, 121787. [[CrossRef](#)] [[PubMed](#)]
23. Karami, P.; Bagheri, H.; Johari-Ahar, M.; Khoshshafar, H.; Arduini, F.; Afkhami, A. Dual-Modality Impedimetric Immunosensor for Early Detection of Prostate-Specific Antigen and Myoglobin Markers Based on Antibody-Molecularly Imprinted Polymer. *Talanta* **2019**, *202*, 111–122. [[CrossRef](#)] [[PubMed](#)]
24. Fang, Q.; Lin, Z.; Lu, F.; Chen, Y.; Huang, X.; Gao, W. A Sensitive Electrochemiluminescence Immunosensor for the Detection of PSA Based on CdWS Nanocrystals and Ag + @UIO-66-NH<sub>2</sub> as a Novel Coreaction Accelerator. *Electrochim. Acta* **2019**, *302*, 207–215. [[CrossRef](#)]
25. Zhang, M.; Hu, X.; Mei, L.; Zhang, L.; Wang, X.; Liao, X.; Qiao, X.; Hong, C. PSA Detection Electrochemical Immunosensor Based on MOF-235 Nanomaterial Adsorption Aggregation Signal Amplification Strategy. *Microchem. J.* **2021**, *171*, 106870. [[CrossRef](#)]
26. Liu, X.P.; Chang, N.; Chen, J.S.; Mao, C.J.; Jin, B.K. Ultrasensitive Photoelectrochemical Immunosensor Based on a G-C<sub>3</sub>N<sub>4</sub>/SnS<sub>2</sub> Nanocomposite for Prostate-Specific Antigen Detection. *Microchem. J.* **2021**, *168*, 106337. [[CrossRef](#)]
27. Feng, J.; Li, Y.; Li, M.; Li, F.; Han, J.; Dong, Y.; Chen, Z.; Wang, P.; Liu, H.; Wei, Q. A Novel Sandwich-Type Electrochemical Immunosensor for PSA Detection Based on PtCu Bimetallic Hybrid (2D/2D) RGO/g-C<sub>3</sub>N<sub>4</sub>. *Biosens. Bioelectron.* **2017**, *91*, 441–448. [[CrossRef](#)] [[PubMed](#)]
28. Kavosi, B.; Salimi, A.; Hallaj, R.; Moradi, F. Ultrasensitive Electrochemical Immunosensor for PSA Biomarker Detection in Prostate Cancer Cells Using Gold Nanoparticles/PAMAM Dendrimer Loaded with Enzyme Linked Aptamer as Integrated Triple Signal Amplification Strategy. *Biosens. Bioelectron.* **2015**, *74*, 915–923. [[CrossRef](#)] [[PubMed](#)]
29. Kim, D.J.; Lee, N.E.; Park, J.S.; Park, I.J.; Kim, J.G.; Cho, H.J. Organic Electrochemical Transistor Based Immunosensor for Prostate Specific Antigen (PSA) Detection Using Gold Nanoparticles for Signal Amplification. *Biosens. Bioelectron.* **2010**, *25*, 2477–2482. [[CrossRef](#)]
30. Wei, Y.; Li, X.; Sun, X.; Ma, H.; Zhang, Y.; Wei, Q. Dual-Responsive Electrochemical Immunosensor for Prostate Specific Antigen Detection Based on Au-CoS/Graphene and CeO<sub>2</sub>/Ionic Liquids Doped with Carboxymethyl Chitosan Complex. *Biosens. Bioelectron.* **2017**, *94*, 141–147. [[CrossRef](#)]
31. Gutiérrez-Zúñiga, G.G.; Hernández-López, J.L. Sandwich-Type ELISA Impedimetric Immunosensor for Early Detection of Prostate-Specific Antigen (PSA) in Human Serum. *Procedia Chem.* **2014**, *12*, 47–54. [[CrossRef](#)]
32. Suresh, L.; Brahman, P.K.; Reddy, K.R.; Bondili, J.S. Development of an Electrochemical Immunosensor Based on Gold Nanoparticles Incorporated Chitosan Biopolymer Nanocomposite Film for the Detection of Prostate Cancer Using PSA as Biomarker. *Enzyme Microb. Technol.* **2018**, *112*, 43–51. [[CrossRef](#)] [[PubMed](#)]
33. Filik, H.; Avan, A.A. Nanostructures for Nonlabeled and Labeled Electrochemical Immunosensors: Simultaneous Electrochemical Detection of Cancer Markers: A Review. *Talanta* **2019**, *205*, 120153. [[CrossRef](#)] [[PubMed](#)]

34. Iannazzo, D.; Espro, C.; Celesti, C.; Ferlazzo, A.; Neri, G. Smart Biosensors for Cancer Diagnosis Based on Graphene Quantum Dots. *Cancers* **2021**, *13*, 3194. [[CrossRef](#)] [[PubMed](#)]
35. Li, L.; Wei, Y.; Zhang, S.; Chen, X.; Shao, T.; Feng, D. Electrochemical Immunosensor Based on Metal Ions Functionalized CNSs@Au NPs Nanocomposites as Signal Amplifier for Simultaneous Detection of Triple Tumor Markers. *J. Electroanal. Chem.* **2021**, *880*, 114882. [[CrossRef](#)]
36. Wang, N.; Wang, J.; Zhao, X.; Chen, H.; Xu, H.; Bai, L.; Wang, W.; Yang, H.; Wei, D.; Yuan, B. Highly Sensitive Electrochemical Immunosensor for the Simultaneous Detection of Multiple Tumor Markers for Signal Amplification. *Talanta* **2021**, *226*, 122133. [[CrossRef](#)]
37. Zheng, Y.; Li, J.; Zhou, B.; Ian, H.; Shao, H. Advanced Sensitivity Amplification Strategies for Voltammetric Immunosensors of Tumor Marker: State of the Art. *Biosens. Bioelectron.* **2021**, *178*, 113021. [[CrossRef](#)]
38. Cho, H.Y.; Choi, J.H.; Lim, J.; Lee, S.N.; Choi, J.W. Microfluidic Chip-Based Cancer Diagnosis and Prediction of Relapse by Detecting Circulating Tumor Cells and Circulating Cancer Stem Cells. *Cancers* **2021**, *13*, 1385. [[CrossRef](#)]
39. Regiart, M.; Fernández-Baldo, M.A.; Spotorno, V.G.; Bertolino, F.A.; Raba, J. Ultra Sensitive Microfluidic Immunosensor for Determination of Clenbuterol in Bovine Hair Samples Using Electrodeposited Gold Nanoparticles and Magnetic Micro Particles as Bio-Affinity Platform. *Biosens. Bioelectron.* **2013**, *41*, 211–217. [[CrossRef](#)]
40. Regiart, M.; Fernández-Baldo, M.A.; Villarroel-Rocha, J.; Messina, G.A.; Bertolino, F.A.; Sapag, K.; Timperman, A.T.; Raba, J. Microfluidic Immunosensor Based on Mesoporous Silica Platform and CMK-3/Poly-Acrylamide-Co-Methacrylate of Dihydrolipoic Acid Modified Gold Electrode for Cancer Biomarker Detection. *Anal. Chim. Acta* **2017**, *963*, 83–92. [[CrossRef](#)]
41. Zhang, J.; Chua, S.L.; Khoo, B.L. Worm-Based Microfluidic Biosensor for Real-Time Assessment of the Metastatic Status. *Cancers* **2021**, *13*, 873. [[CrossRef](#)]
42. Chan, K.M.; Gleadle, J.M.; Gregory, P.A.; Phillips, C.A.; Safizadeh Shirazi, H.; Whiteley, A.; Li, J.; Vasilev, K.; Macgregor, M. Selective Microfluidic Capture and Detection of Prostate Cancer Cells from Urine without Digital Rectal Examination. *Cancers* **2021**, *13*, 5544. [[CrossRef](#)] [[PubMed](#)]
43. Panini, N.V.; Messina, G.A.; Salinas, E.; Fernández, H.; Raba, J. Integrated Microfluidic Systems with an Immunosensor Modified with Carbon Nanotubes for Detection of Prostate Specific Antigen (PSA) in Human Serum Samples. *Biosens. Bioelectron.* **2008**, *23*, 1145–1151. [[CrossRef](#)] [[PubMed](#)]
44. Hou, L.; Huang, J.; Liu, S.; Lin, T.; Zhao, S. Magneto-Controlled Fluorescent Immunosensor for Sensitive Determination of Biomarker via Three-Dimensional AuNCs/Liposome Networks. *Sens. Actuators B Chem.* **2021**, *342*, 130075. [[CrossRef](#)]
45. Barry, M.J. Clinical practice. Prostate-specific-antigen testing for early diagnosis of prostate cancer. *N. Engl. J. Med.* **2001**, *344*, 1373–1377. [[CrossRef](#)] [[PubMed](#)]
46. Triroj, N.; Jaroenapibal, P.; Shi, H.; Yeh, J.; Beresford, R. Microfluidic chip-based nanoelectrode array as miniaturized biochemical sensing platform for prostate-specific antigen detection. *Biosens. Bioelectron.* **2011**, *26*, 2927–2933. [[CrossRef](#)] [[PubMed](#)]
47. Chikkaveeraiah, B.V.; Mani, V.; Patel, V.; Gutkind, J.S.; Rusling, J.F. Microfluidic electrochemical immunoarray for ultrasensitive detection of two cancer biomarker proteins in serum. *Biosens. Bioelectron.* **2011**, *26*, 4477–4483. [[CrossRef](#)] [[PubMed](#)]
48. Tang, C.; Vaze, A.; Shen, M.; Rusling, J.F. High-Throughput Electrochemical Microfluidic Immunoarray for Multiplexed Detection of Cancer Biomarker Proteins. *ACS Sensors* **2016**, *1*, 1036–1043. [[CrossRef](#)]
49. Zhu, C.; Yang, G.; Li, H.; Du, D.; Lin, Y. Electrochemical sensors and biosensors based on nanomaterials and nanostructures. *Am. Chem. Soc.* **2015**, *87*, 230–249. [[CrossRef](#)]
50. Saem, S.; Zhu, Y.; Luu, H.; Moran-Mirabal, J. Bench-Top Fabrication of an All-PDMS Microfluidic Electrochemical Cell Sensor Integrating Micro/Nanostructured Electrodes. *Sensors* **2017**, *17*, 732. [[CrossRef](#)]
51. Barbosa, A.I.; Gehlot, P.; Sidapra, K.; Edwards, A.D.; Reis, N.M. Portable smartphone quantitation of prostate specific antigen (PSA) in a fluoropolymer microfluidic device. *Biosens. Bioelectron.* **2015**, *70*, 5–14. [[CrossRef](#)]
52. Mavrikou, S.; Moschopoulou, G.; Zafeirakis, A.; Kalogeropoulou, K.; Giannakos, G.; Skevis, A.; Kintzios, S. An Ultra-Rapid Biosensory Point-of-Care (POC) Assay for Prostate-Specific Antigen (PSA) Detection in Human Serum. *Sensors* **2018**, *18*, 3834. [[CrossRef](#)] [[PubMed](#)]
53. Srinivasan, B.; Nanus, D.M.; Erickson, D.; Mehta, S. Highly Portable Quantitative Screening Test for Prostate-Specific Antigen at Point of Care. *Curr. Res. Biotechnol.* **2021**, *3*, 288–299. [[CrossRef](#)] [[PubMed](#)]
54. Traynor, S.M.; Pandey, R.; Maclachlan, R.; Hosseini, A.; Didar, T.F.; Li, F.; Soleymani, L. Review—Recent Advances in Electrochemical Detection of Prostate Specific Antigen (PSA) in Clinically-Relevant Samples. *J. Electrochem. Soc.* **2020**, *167*, 037551. [[CrossRef](#)]